# Cascaded holographic polymer reflection grating filters for optical-code-division multiple-access applications

Raymond K. Kostuk, Wendi Maeda, Chia-Hung Chen, Ivan Djordjevic, and Bane Vasic

We evaluate the use of edge-illuminated holographic Bragg filters formed in phenanthrenequinone-doped poly(methyl methacrylate) for optical-code-division multiple-access (OCDMA) coding and decoding applications. Experimental cascaded Bragg filters are formed to select two different wavelengths with a fixed distance between the gratings and are directly coupled to a fiber-measurement system. The configuration and tolerances of the cascaded gratings are shown to be practical for time–wavelength OCDMA applications. © 2005 Optical Society of America

*OCIS codes:* 060.0060, 060.4510, 090.0090, 090.7370.

## 1. Introduction

Edge-illuminated holographic Bragg filters (EIHBFs) have a variety of advantages for fiber communication systems.[1–3] They can be formed in low-cost polymers with visible rather than UV illumination, as is required for fiber Bragg gratings. The optics and optical sources required for visible recording are less expensive than UV optics and sources. Since the filters are Bragg reflection gratings they are not sensitive to polarization. EIHBFs are essentially free-space optical devices; therefore the beam does not experience a shift in Bragg wavelengths between the core and the cladding regions as in fiber Bragg gratings. It is possible to record EIHBFs in voltage-controlled liquid-crystal materials, providing active switching that does not depend on mechanical thermal expansion or stretching techniques.[4,5]

Optical-code-division multiple access (OCDMA) is another important multiplexing scheme for increasing the spectral efficiency of fiber communication systems.[6,7] The advantages of OCDMA include asynchronous multiple access with 1:1 or 1:$N$ access and routing operations without the need for optical switches. It can also accommodate different optical bandwidth assignments. A variety of coding methods for OCDMA have been proposed, including encoding and decoding the wavelength, time, or phase of the optical signal.

Phenanthrenequinone- (PQ-) doped poly(methyl methacrylate) (PMMA) is an attractive material for making holographic Bragg filters. The material can be used to make thick samples that can be molded into different forms, and it has a reasonably high efficiency at telecommunication wavelengths. PQ-doped PMMA can be formulated for minimal shrinkage and refractive index change after processing.[8,9] In addition, polymers are relatively inexpensive to fabricate and can be synthesized with other compounds to enhance their diffraction efficiency and transmission properties.[10]

In previous work, cascaded grating filters were recorded in fibers for OCDMA encoders and decoders,[11,12] and multiplexed wavelength filters and apodized grating filters were formed in a polymer edge-illuminated hologram configuration.[1–3] In this paper we describe the design and fabrication of polymer-cascaded edge-illuminated holographic wavelength filters at 1550 nm with fixed spacing between gratings for use as OCDMA encoders and decoders. The reflectance signals are coupled into a fiber communication system, and the bit error rate (BER) as a function of wavelength is monitored to determine cross talk between adjacent wavelength chips. To our knowledge these experiments represent the first demonstration of cascaded polymer holographic gratings with different reflectance bands and time delays between grating elements, which is a first step toward realizing a polymer OCDMA encoder–decoder.

The authors are with the Electrical and Computer Engineering Department, University of Arizona, Tucson, Arizona 85721. R. K. Kostuk's e-mail address is kostuk@ece.arizona.edu.

Received 16 May 2005; accepted 8 August 2005.
0003-6935/05/357581-06$15.00/0

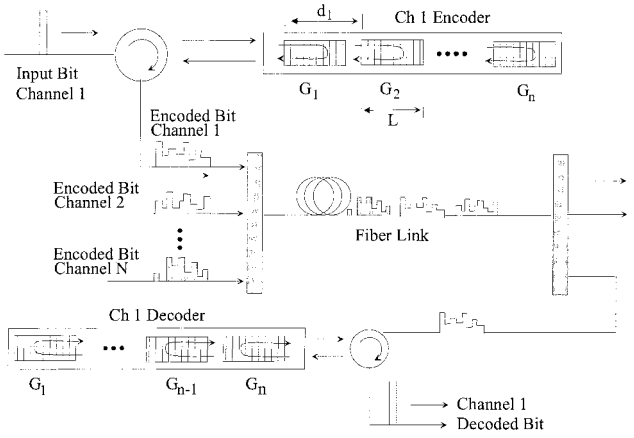


Fig. 1. Asynchronous OCDMA system for encoding and decoding wavelength–time codes. A broadband input signal enters the encoder that consists of grating elements ($G_n$) separated by distances ($d_m$).

## 2. Wavelength–Time-Encoded OCDMA

One method of forming wavelength–time-coded OCDMA encoders and decoders is to cascade multiple gratings with a fixed separation between gratings along the direction of beam propagation.[11,12] An arrangement for this device is illustrated in Fig. 1. The number of simultaneous users that can be accommodated on the optical channel is a function of the number of $\lambda$–$t$ slots or chips that can be cascaded in the encoder–decoder pair. Therefore the technique used to implement the encoder–decoder must be capable of incorporating a large number of $\lambda$–$t$ chips.

The number of users supported by an incoherent multidimensional OCDMA system is proportional to the product of the code dimensions. Therefore in a wavelength–time code with $N$ wavelength and $M$ time-delay chips the number of users or cardinality $\Phi$ is[13]

$$\Phi \propto N(NM - 1). \tag{1}$$

The number of wavelength chips that is available can be determined from

$$N = \frac{\Delta\lambda}{\delta\lambda}, \tag{2}$$

and the number of time-delay chips is

$$M = \frac{\Delta T}{\delta t}, \tag{3}$$

where $\Delta\lambda$ is the available spectral bandwidth of the source, $\delta\lambda$ is the spectral bandwidth of a filter element, $\Delta T$ is the time corresponding to a bit period ($B = 1/\Delta T$), and $\delta t$ is the minimum resolvable time delay. These simple relations indicate that, for a fixed bit period, devices used for encoders and decoders should minimize $\delta\lambda$ and $\delta t$ and maximize $\Delta T$. For a 10 Gbit/s system $\Delta T = 100$ ps and corresponds to a propagation distance of 2 cm in a material with a refractive index of 1.5. For an encoder or decoder operating in a cascaded reflection mode, the available effective length for cascaded elements is reduced by a factor of 2 to 1 cm. This is the geometrical length into which spectral and temporal chips for the code must be incorporated.

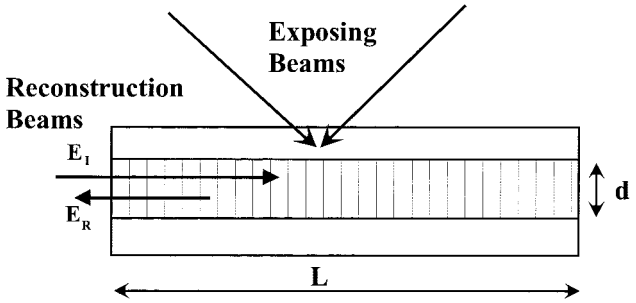


Fig. 2. Edge-illuminated hologram configuration. The exposing beams are from the side of the material allowing apodized grating profiles and formation by use of a transmission grating configuration. $E_i$, incident-beam direction; $E_r$, reflected-beam direction; $L$, grating length in the reflection mode; $d$, material thickness.

## 3. Edge-Illuminated Hologram Design for OCDMA Encoders–Decoders

The basic configuration for an edge-illuminated hologram is shown in Fig. 2. The holograms are formed as transmission gratings and reconstructed in reflection mode by illumination of the recording material from an edge. This allows a great deal of flexibility in the filter design to realize apodized and cascaded gratings, minimal effects that are due to material change during processing, and polarization-insensitive performance.

The diffraction efficiency of an unslanted reflection grating can be determined with the Kogelnik coupled-wave model[14] for a dielectric reflection grating with a loss of

$$\eta = SS^*, \tag{4}$$

where

$$S = j\frac{\sinh(\nu\cosh a)}{\cosh(a + \nu\cosh a)},$$

$$\nu = \frac{\pi\Delta nL}{\lambda_{\text{Bragg}}},\ \xi = \alpha L + j\frac{\vartheta L}{2},\ a = \sinh^{-1}(\xi/\nu).$$

The refractive index modulation is $\Delta n$, the grating length is $L$, the Bragg wavelength is $\lambda_{\text{Bragg}}$, and the absorption is $\alpha$. The dephasing term $\vartheta$ gives a measure of the deviation in reconstruction parameters from the Bragg condition. If we consider only a wavelength deviation $\Delta\lambda$ from the Bragg wavelength, the dephasing term is

$$\vartheta = \frac{K^2\Delta\lambda}{4\pi n}, \tag{5}$$

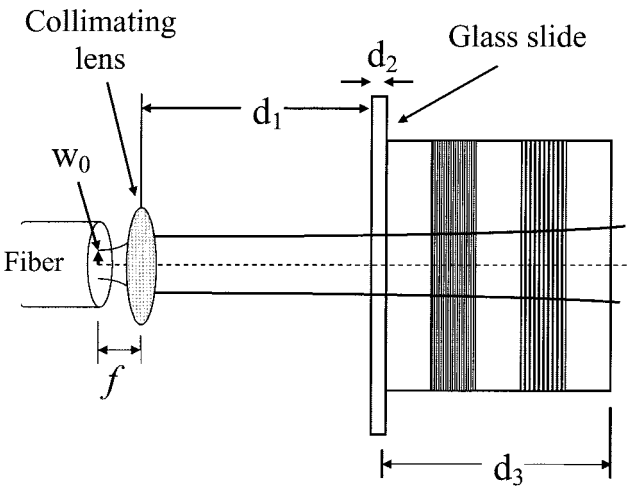


Fig. 3. Coupling from a fiber into the cascaded grating substrate: $f$, focal length of the lens; $w_0$, $1/e^2$ radius of the beam from the fiber; $d_1$, separation between the lens and the substrate; $d_2$, end glass thickness; $d_3$, length of the polymer.

where $K = 2\pi/\Lambda$, $\Lambda$ is the grating vector, and $n$ is the refractive index of the material. The required grating-length and index-modulation combination for achieving a specific reflection efficiency can be estimated from Eq. (5). If it can be assumed that $\Delta n \ll \lambda/L$, the corresponding spectral bandwidth can be determined from the approximate relation[15]

$$\Delta\lambda = \frac{\lambda^2}{nL}. \tag{6}$$

For typical operating parameters of $\lambda = 1.55$ μm and $n = 1.50$, the relation is $L = 1.602 \times 10^3/\Delta\lambda$ μm, where $\Delta\lambda$ is in nanometers. Therefore, for $\Delta\lambda = 0.2$ nm, $L = 8$ mm. Using this length in the diffraction efficiency relationship with $\eta = 0.98$ results in an estimate for $\Delta n = 1.631 \times 10^{-4}$. This value is consistent with previously published data for the refractive index modulation obtained in PQ-doped PMMA.[3,9]

This result provides guidance for the type of system in which polymer edge-illuminated holograms can be used. For instance, the discussion in the previous section concluded that the maximum length for a cascaded OCDMA encoder–decoder operating at 10 Gbits/s in a reflection mode is approximately 1 cm. Therefore only one grating with a 0.2 nm bandwidth can fit within this length constraint and would not provide a useful code sequence. If the spectral bandwidth of the grating is increased to 0.8 nm and the modulation bands reduced to 2.5 Gbit/s the required grating length can be reduced to 2 mm and the overall length in reflection mode to store a code is increased to 2.5 cm. This configuration can accommodate codes that are much more complex. For instance, dividing the available encoder–decoder length (25 mm) into spectral and time chips with 2 mm segments will allow up to 12 wavelengths and time-delay chips. A 2.5 Gbit/s bit rate and 0.8 nm spectral bandwidth is appropriate for metropolitan-area network applications[16] and suggests a useful system level for polymer CDMA devices.

Because the edge-illuminated hologram is not a waveguide device, the beam expansion in relation to the thickness of the polymer must be considered to ensure that the beam does not extend beyond the limits of the material. The cascaded grating device is coupled to a fiber by a fiber collimator attached to the output end of the fiber, as illustrated in Fig. 3. The fiber collimator used for our measurements is model F-M5-S-1550-4.6 from Newport that has a 4.6 mm effective focal length. An analysis of the Gaussian beam expansion for this system[17] with a single-mode fiber operating at 1550 mm with a diameter of 8 μm shows that less than 1% of the incident-beam power is lost on coupling back into the launch fiber.

## 4. Experimental Cascaded Gratings

To demonstrate the use of polymer holograms for OCDMA encoders and decoders, edge-illuminated hologram samples were formed in 1.65 mm thick samples of PQ-doped PMMA by use of a bulk polymerization process.[8,9] The basic process consisted of mixing a liquid solution containing MMA, 2,2′-azobis(2-methylpropionitrile), and PQ in a weight ratio of 100:0.5:0.7 and then pouring the solution into a mold. Next the samples were heated at 50 °C for 120 h to thermally activate polymerization and solidify the liquid, and then they were cut into 5 cm × 5 cm squares. The absorption constant of the resulting material was measured with a spectrophotometer and found to be 0.009/mm at 632.8 nm and 0.014/mm at 1550 nm for both the unexposed and the exposed samples. The refractive index of the material was found to be 1.488 at 632.8 nm and 1.479 at 1550 nm by use of a prism coupler.

The gratings were written in a transmission configuration (Fig. 2) by an argon-ion laser at a wavelength of 488 nm with an exposure energy of 2000 mJ/cm$^2$. Two gratings with different grating periods were written in a cascaded arrangement by use of a mask, as illustrated in Fig. 4, to set the lengths of the gratings and the separation distance between the gratings. The grating aperture was fixed at 10 mm, and a separation of 15 or 20 mm was used for different samples. The separation lengths corresponded to time delays of 148 and 197 ps in the polymer. The gratings were formed in an unslanted transmission configuration by exposing one clear area of the mask with two interfering plane waves at 488 nm while the second clear area was kept covered. The sample was then translated on a micropositioning stage, and the second exposure was made with a different interbeam angle to form a grating with a different period. The angles of the two exposing beams relative to the normal to the hologram substrate were calculated according to the Bragg relation for unslanted gratings:

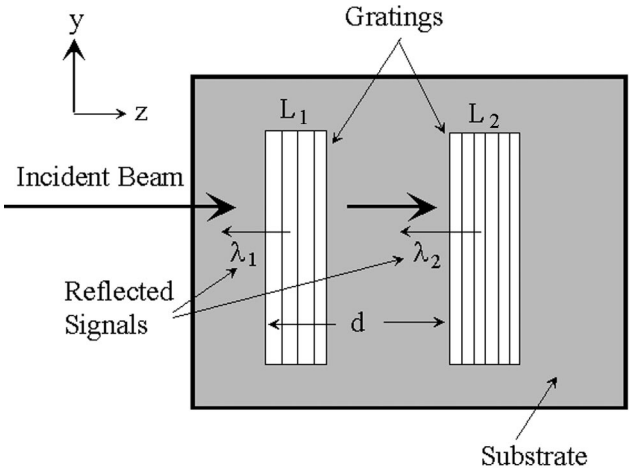


Fig. 4. Mask layout used for forming the cascaded gratings: $L_1$, $L_2$, lengths of the gratings; $\lambda_1$, $\lambda_2$, corresponding filtered wavelengths; $d$, separation between gratings.

$$\theta = \sin^{-1}\left(\frac{\lambda_{488}}{2n_{488}\Lambda}\right). \quad (7)$$

Holograms were fabricated with grating periods of 522.5, 525.2, and 528.0 nm to match wavelengths corresponding to the International Telecommunication Union (ITU) grid points 1544.53, 1552.52, and 1560.61 nm. The angles of the exposing beams were established by retroreflecting each beam back to the pinhole of the spatial filter and noting the angle mark on a high-precision rotation stage with 0.001° positioning accuracy (Newport model 495CC with an ESP 300 Universal Motion Controller). The difference between the angle marks measured on the rotation stage was adjusted to equal a value of $2\theta$ that matches a specific grating period and ITU wavelength. The accuracy of this recording process was found to be approximately 1 nm and was limited by the requirement to reposition the construction beams between exposures.

After exposure, the samples were kept in a dark enclosure for 24 h to enhance the grating strength. To terminate the diffusion reaction in the material, the samples were fixed by illumination with incoherent blue light. After processing, the edges of the grating substrate were polished and glass coverslips were cemented onto the edges, forming an optical-quality interface. The orientation of the sample was changed to an edge-illuminated configuration to measure the reflectance, as shown in Figs. 2 and 3.

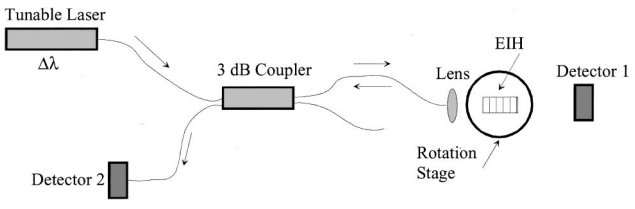


Fig. 5. System used to measure the reflection characteristics of the cascaded polymer gratings: EIH, edge-illuminated hologram; $\Delta\lambda$, tuning range of the tunable laser in the 1550 nm bandwidth region.

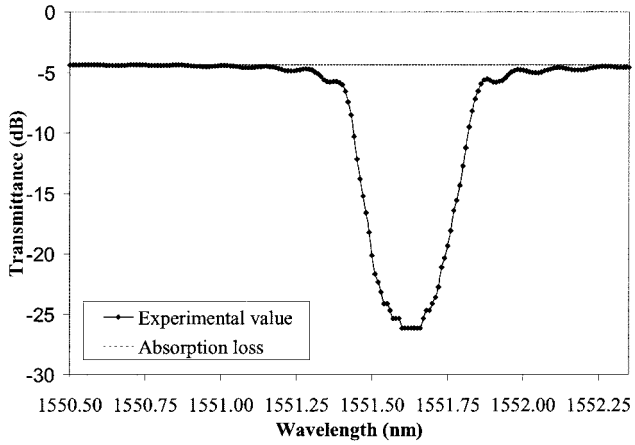


Fig. 6. Transmittance of one of the cascaded gratings experimentally measured by Detector 1 in the system described in Fig. 5.

Figure 5 illustrates the fiber-optic system used for measuring the reflectance of the gratings. A tunable laser operating in the 1550 nm spectral range with 0.01 nm tuning accuracy is connected to a $2 \times 2$, 3 dB coupler, with one of the outputs connected to a collimating lens and the sample and the return signal monitored with a detector. The beam enters the edge of the sample, is reflected from the gratings, and reenters the lens and fiber. The sample is mounted on a tilt–tip–rotation stage to allow fine alignment adjustments. A second detector is placed on the opposite side of the grating substrate to monitor the transmittance of the sample. A reference signal for determining the hologram reflection efficiency is obtained by replacement of the cascaded holograms with a near-IR mirror mounted on the tilt–tip–rotation stage. This also allows the removal of any backreflections from other components in the system and the unused fiber in the 3 dB coupler.

Figure 6 shows the transmittance spectrum for one of the 5 cm long samples, and Fig. 7 shows the reflection spectrum measured for a sample designed for peak reflectance signals at 1544.5 and 1552.5 nm. The

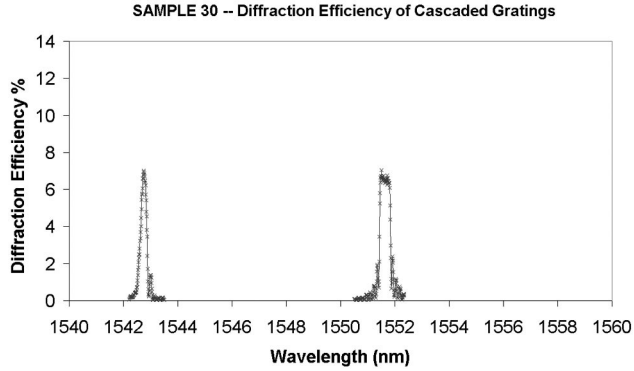


Fig. 7. Measured reflection efficiency for two wavelengths coupled back into a single-mode launch fiber as measured with Detector 2 in Fig. 5.

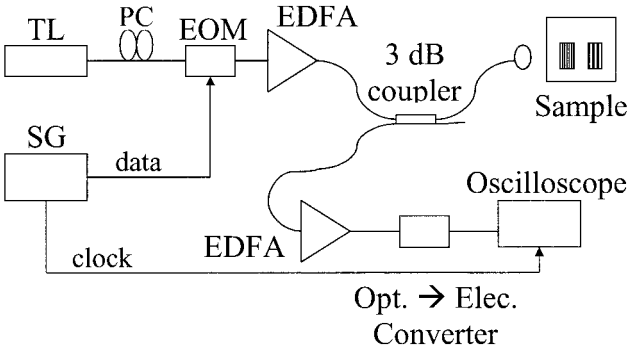


Fig. 8. System for measuring the eye diagram with the signal reflected from the cascaded polymer grating: TL, tunable laser; PC, polarization controller; EOM, electro-optic modulator; EDFA, erbium-doped fiber amplifier; SG, signal generator.

measured wavelengths differ from the design wavelengths by approximately 1 nm and are primarily due to the technique for setting the angles of the exposure beams. This can be corrected either by use of a more accurate alignment process or phase masks to form the construction beams in one exposure. The reflected signal coupled back into a single-mode fiber is low (~10%). However, the transmittance spectrum for the grating at 1552.5 nm indicates that higher reflected power is possible with improved fiber-coupling techniques.

The time delay between gratings was measured by a comparison of reflected signals on a high-speed oscilloscope by use of the system shown in Fig. 8. For this measurement the reflected signals are coupled back into a single-mode fiber. The procedure consists of first tuning a 1550 nm band laser to the peak reflection wavelength of one of the gratings. A 16 bit sequence consisting of a one followed by 15 zeros is generated with the signal generator. The pulse height of the reflected signal as a function of time is stored on the oscilloscope. The laser is then tuned to the peak reflected signal for the second grating with the same 1:15 bit sequence, and the arrival time is compared with the arrival time from the first grating. The delay times are 125 ps for the 15 mm grating separation and 167 ps for the 20 mm separation. The difference between the calculated and measured delay times is approximately 20 ps and is within the accuracy of our oscilloscope and mask used for these experiments.

The system shown in Fig. 8 was also used to generate an eye diagram with the reflected signals from the cascaded gratings. An eye diagram for the reflection signal at the Bragg wavelength from one of the cascaded gratings at a data rate of 10 Gbits/s is shown in Fig. 9(a). The $Q$ parameter is obtained from this measurement and with the relation

$$Q = \frac{I_1 - I_2}{\sigma_1 + \sigma_2} = 11, \tag{8}$$

where $I_1$ and $I_2$ are the high and low signal levels, respectively, and $\sigma_1$ and $\sigma_2$ are the variances of the high and low signal levels, respectively. $Q$ parameters of this magnitude result in BERs of

$$\mathrm{BER} = \frac{1}{\sqrt{2\pi}} \exp(-Q^2/2) = 1.93 \times 10^{-28} \tag{9}$$

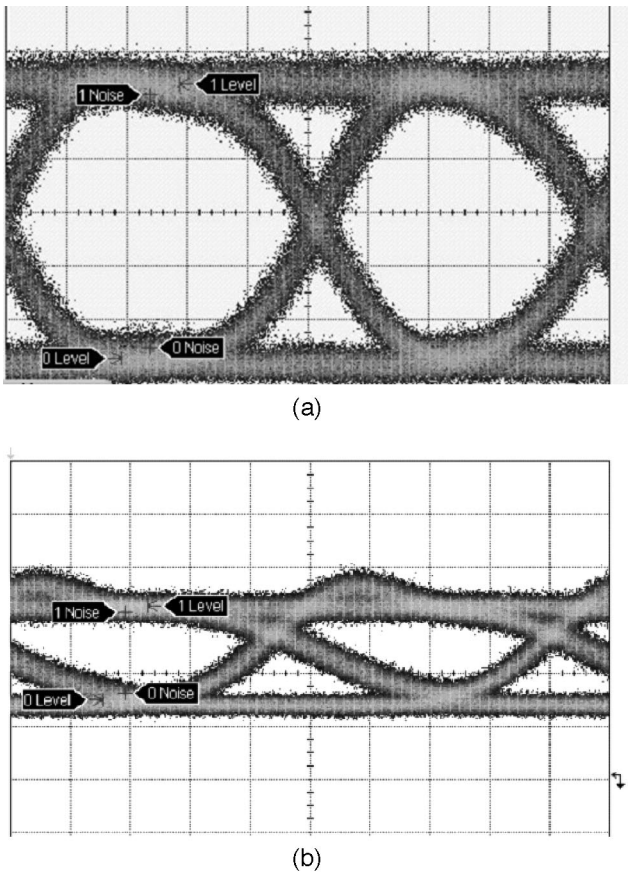


Fig. 9. (a) Eye diagram generated by the reflected signal when the incident wavelength is tuned to the Bragg wavelength of one of the cascaded gratings. (b) Eye diagram generated by the reflected signal when the wavelength is tuned approximately 0.2 nm from the Bragg wavelength for the grating.

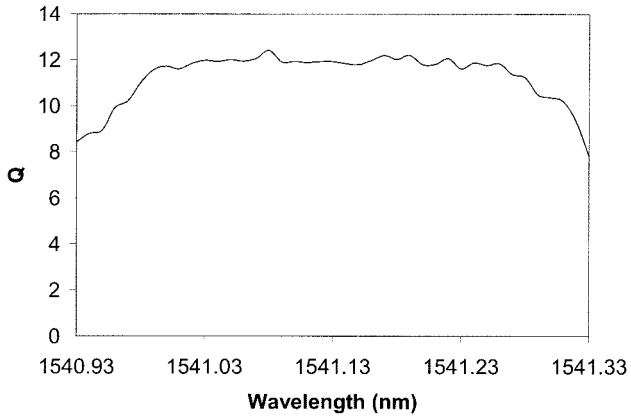


Fig. 10. Signal $Q$ as a function of wavelength determined from the eye diagrams of the signals reflected from one of the polymer gratings and coupled back into a single-mode fiber by use of the system described in Fig. 7.

with good system performance capability. The change in BER with variation from the design wavelength is also an important measurement as it indicates how sensitive the device is to source manufacturing and degradation tolerances. Figure 9(b) shows the degradation of the eye diagram as the wavelength is detuned from the Bragg wavelength, and Fig. 10 shows the corresponding change in $Q$ with deviation from the design wavelength of the grating. These results indicate that the gratings retain good performance with $Q \geq 8.5$ (BER $\sim 10^{-16}$) with wavelength variations of $\Delta\lambda \leq \pm 0.20$ nm.

## 5. Conclusion

In this paper we have evaluated the use of polymer edge-illuminated holograms for encoders and decoders in CDMA optical fiber communication systems. Basic design constraints resulting from grating efficiency, spectral bandwidth, and separation were considered for different bit-rate communication systems. This analysis suggests that edge-illuminated holographic CDMA encoders and decoders would be useful for codes with approximately ten wavelengths and time chips for systems operating at 2.5 Gbits/s.

The concept of cascaded edge-illuminated holograms has been demonstrated by fabricating elements in PQ-doped PMMA polymer materials. The gratings formed had a spectral bandwidth of ~0.4 nm and a measured time delay between gratings of ~125 ps. The gratings were coupled into a fiber-communication system and allowed system measurements by use of reflection signals from the cascaded gratings. The resulting BER and spectral bandwidth dependence of the reflection signals were also found to be tolerant of system variations that were due to manufacturing and degradation.

The limiting factors of PQ MMA polymer edge-illuminated holograms for use in CDMA encoders and decoders are the material loss (0.02/mm) and fiber-coupling efficiency. Material loss can be reduced by fluorination or partial halogenation of the polymer,[10] and fiber-coupling losses can be reduced by improved packaging methods. The accuracy of wavelength selection and time delay can be improved by use of lithographically formed phase masks with accurate aperture and separation dimensions to form the writing beams.

The demonstration of cascaded gratings in low-cost polymers as illustrated in this work suggests the possibility of using OCDMA techniques to extend the performance of metropolitan and local-area networks.

The authors thank the National Science Foundation, grant ANI-0325979, for supporting this work.

## References

1. A. Sato, M. Scepanovic, and R. K. Kostuk, "Holographic edge-illuminated polymer Bragg gratings for dense wavelength division optical filters at 1550 nm," Appl. Opt. **42,** 778–784 (2003).
2. A. Sato and R. K. Kostuk, "Holographic gratings for dense wavelength division optical filters at 1550 nm using phenanthrenquinone doped poly methyl methacrylate," in Proc. SPIE **5216,** 44–52 (2003).
3. O. Beyer, I. Nee, F. Havermeyer, and K. Buse, "Holographic recording of Bragg gratings for wavelength division multiplexing in doped and partially polymerized poly(methyl methacrylate)," Appl. Opt. **42,** 30–37 (2003).
4. S. Yeralan, J. Gunther, D. Ritums, R. Cid, and M. Popovich, "Switchable Bragg grating devices for telecommunications applications," Opt. Eng. **41,** 1774–1779 (2002).
5. T. J. Bunning, L. V. Natarajan, V. P. Tondiglia, and R. L. Sutherland, "Holographic polymer dispersed liquid crystals (H-PDLCs)," Annu. Rev. Mater. Sci. **30,** 83–115 (2000).
6. T. W. Mossberg and M. G. Raymer, "Optical code-division multiplexing: The intelligent optical solution," Opt. Photon. News **12**(3), 50–54 (2001).
7. J. Shah, "Optical CDMA," Opt. Photon. News **14**(4), 42–47 (2003).
8. G. J. Steckman, I. Solomatine, G. Zhou, and D. Psaltis, "Characterization of phenanthrenequinone-doped poly(methyl methacrylate) for holographic memory," Opt. Lett. **23,** 1310–1312 (1998).
9. K. Y. Hsu, S. H. Lin, Y.-N. Hsiao, and W. T. Whang, "Experimental characterization of phenanthrenequinone doped poly(methyl methacrylate) photopolymer for volume holographic storage," Opt. Eng. **42,** 1390–1396 (2003).
10. L. Eldada and L. W. Shacklette, "Advances in polymer integrated optics," IEEE J. Sel. Top. Quantum Electron. **6,** 54–68 (2000).
11. S. La Rochelle, P.-Y. Cortes, H. Fathallah, L. A. Rusch, and H. B. Jaafar, "Writing and applications of fiber Bragg grating arrays," in Proc. SPIE **4087,** 140–149 (2000).
12. A. Grunnet-Jepsen, A. E. Johnson, E. S. Maniloff, T. W. Mossberg, M. J. Munroe, and J. N. Sweetser, "Fiber Bragg grating based spectral encoder/decoder for lightwave CDMA," Electron. Lett. **35,** 1096–1097 (1999).
13. G.-C. Yang and W. C. Kwong, *Prime Codes with Applications to CDMA Optical and Wireless Networks* (Artech House, 2002).
14. H. Kogelnik, "Coupled wave theory for thick hologram gratings," Bell Syst. Tech. J. **48,** 2909–2946 (1969).
15. T. Erdogan, "Fiber grating spectra," J. Lightwave Technol. **15,** 1277–1294 (1997).
16. R. P. Braun, "Cost effective metro networks," in the *16th Annual Meeting of the Lasers and Electro-Optics Society* (IEEE, 2003), paper WQ1, pp. 610–611.
17. J. T. Verdeyen, *Laser Electronics,* 3rd ed. (Prentice-Hall, 1995), pp. 63–85.